Journal of Enzyme Inhibition and Medicinal Chemistry, 2011; 26(1): 37–45

ISSN 1475-6366 print/ISSN 1475-6374 online
DOI: 10.3109/14756361003671060

informa
healthcare

RESEARCH ARTICLE

Synthesis and antiproliferative activities against Hep-G2 of salicylanide derivatives: potent inhibitors of the epidermal growth factor receptor (EGFR) tyrosine kinase

Zhen-Wei Zhu, Lei Shi, Xiao-Ming Ruan, Ying Yang, Huan-Qiu Li, Suo-Ping Xu, and Hai-Liang Zhu

State Key Laboratory of Pharmaceutical Biotechnology, Nanjing University, Nanjing 210093, People's Republic of China

Abstract

A series of salicylanilide derivatives (compounds **1**–**32**) were synthesised by reacting substituted salicylic acids and anilines. The chemical structures of these compounds were determined by ^{1}H-NMR, electrospray ionisation mass spectrometry (ESI-MS) and elemental analysis. The compounds were assayed for their antiproliferative activities against the *Hep-G2* cell line by the 3-(4,5-dimethylthylthiazol-2-yl)-2,5-diphenyltetrazolium bromide (MTT) method. Among the compounds tested, **22** and **28** showed the most favouable antiproliferative activities with 50% inhibitory concentration (IC_{50}) values of 1.7 and 1.3 μM, respectively, which were comparable to the positive control of 5-fluorouracil (IC_{50} = 1.8 μM). A solid-phase ELISA assay was also performed to evaluate the ability of compounds **1**–**32** to inhibit the autophosphorylation of the epidermal growth factor receptor tyrosine kinase (EGFR TK). Docking simulations of **22** and **28** were carried out to illustrate the binding mode of the molecule into the EGFR active site, and the result suggested that both compounds **22** and **28** could bind the EGFR kinase well.

Keywords: Salicylanilide derivatives; antiproliferative activities; EGFR TK; structure-activity relationship; docking simulations

Introduction

Liver cancer is one of the most threatening diseases in the world today. A study made by the International Agency for Research on Cancer (IARC) indicated that liver cancer was the third common cancer and caused more than 620,000 deaths per year all over the world. There are several drugs for the treatment of liver cancer such as doxorubicin, fluorouracil, cisplatin, and α-interferon, but all of them have serious side effects and therefore limit their clinical applications. Due to the shortage of effective drugs, the discovery of new compounds with potent anti-hepatoma activities is a very important task. Here, we synthesised a series of salicylanilide derivatives (compounds **1**–**32**). Salicylanilides are usually synthesised from substituted salicylic acids and anilines. Salicylanilide derivatives isolated from natural plants have been reported to possess antiproliferative activities against the *Hep-G2* cell line, a type of liver cancer cell often selected for research to test compounds that may possess potent activity for liver cancer treatment [1–3]. Pei-Wen Hsieh et al. reported the isolation of 4-methoxydianthramide B, a salicylanilide derivative, from the traditional Chinese medicinal plant *Dianthus superbus*. The compound 4-methoxydianthramide B showed antiproliferative activities against the *Hep-G2* cancer cell line with a 50% inhibitory concentration (IC_{50}) value of 4.08 μg/mL [4]. This investigation led to the idea that salicylanilide derivatives could possess potential antiproliferative activities against the *Hep-G2* cell line, and by structure activity relationship (SAR), the results may be useful to gain more understanding about the antiproliferative activities of salicylanilide derivatives. In this paper, we report the synthesis of some salicylanilide compounds and their antiproliferative activities against the *Hep-G2* cell line.

Address for Correspondence: Hai-Liang Zhu, State Key Laboratory of Pharmaceutical Biotechnology, Nanjing University, Nanjing 210093, People's Republic of China. Tel.: +86-25-8359 2572; Fax: +86-25-8359 2672; E-mail zhuhl@nju.edu.cn

(Received 29 October 2009; revised 28 December 2009; accepted 07 January 2010)

Docking simulations of compounds **22** and **28** were carried out to give structural insights into the binding mode with epidermal growth factor receptor tyrosine kinase (EGFR TK) [5–8], to illustrate the antiproliferative activities against the *Hep-G2* cancer cell line. Molecules designed to block EGFR TK, a class of potent, selective, ATP-competitive inhibitors of EGFR TK, induced signaling on their own and further degrade to a DNA damaging species, should induce significant cell-killing in tumours [9,10]. The first molecular probe designed to verify the combi-targeting postulates, was shown to strongly block the EGFR TK activity on its own in a short exposure enzyme assay [11,12]. The receptor protein tyrosine kinases played a key role in signal transduction pathways that regulate cell division and differentiation. The interaction of growth factors with these receptors was a necessary event in the normal regulation of cell growth. However, under certain conditions, as a result of overexpression, mutation, or coexpression of the ligand and the receptor, these receptors could become hyperactivated and induce uncontrolled cell proliferation [13]. Among the growth factor receptor kinases, EGFR kinase (also known as erb-B1 or HER-1) was important in cancer deregulation of growth-factor signaling due to that hyperactivation of EGFR was seen in several cancer types [14,15]. Activation of EGFR might be a result of overexpression, mutations resulting in constitutive activation, or autocrine expression of the ligand. EGFR overexpression was often seen in various cancers [16–18]. Compounds that inhibit the kinase activity of EGFR after binding of its cognate ligand were of potential interest as new therapeutic antitumor agents [19,20].

Chemistry

A series of salicylanilides were synthesised by reacting four kinds of substituted salicylic acids and several kinds of substituted anilines (Scheme 1). All the compounds gave satisfactory chemical analysis. The chemical structures of these compounds were determined by ^{1}H-NMR, electrospray ionisation mass spectrometry (ESI-MS) spectra and elemental analyses.

Results and discussion

Biological activity

The in vitro antiproliferative activities of the synthesised salicylanilide derivatives **1**–**32** were studied using the human liver cancer cell line Hep-G2 by applying the 3-(4,5-dimethylthylthiazol-2-yl)-2,5-diphenyltetrazolium bromide (MTT) colorimetric assay. The compounds were tested over a range of concentrations from 0.5 to 300 μM, and the calculated IC50 values i.e. the concentration (μM) of compounds which were able to cause 50% of cell death with respect to the control culture, are reported in Table 2.

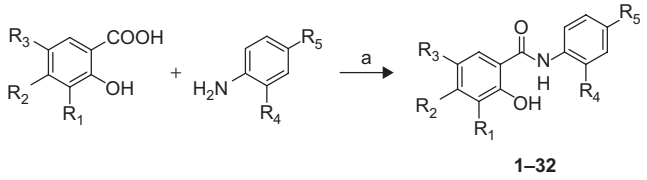

Scheme 1. Synthesis of salicylanilide derivatives **1**–**32**. (a) EDC, CH_2Cl_2, reflux, 8 h, 70–86% yield.

Compounds **1**–**32** could be classed into 4 series: a) salicylic acid series; b) 4-methyl salicylic acid series; c) 5-iodo salicylic acid series; d) 3,5-dibromo salicylic acid series (Table 1). Among these salicylanilide derivatives tested, compounds **22** and **28** were found to show the most potent activities with IC50 values of 1.8 and 1.3 μM, respectively. Compounds **21**, **24**, **25**, **26**, **27**, **30**, **31** and **32** showed the best antiproliferative activities with IC50 values ranging from 5-50 μM. The remaining compounds showed weak antiproliferative activities with IC50 values ranging from 50–300 μM (compounds **2**–**7**, **9**–**12**, **14**, **15**, **18**, **19** and **29**), or not active with IC50 values over 300 μM (compounds **1**, **8**, **13**, **16**, **17**, **20**, **23**).

Compounds **1**–**32** were evaluated for their ability to inhibit the autophosphorylation of EGFR kinases using a solid-phase ELISA assay. A number of the synthesised compounds showed potent EGFR inhibitory activities. The results showed the same trends for antiproliferative activities against Hep-G2 as EGFR was an important factor in liver cancer. (Table 2). Here, again, compounds **22** and **28** showed the most potent inhibitory activities (IC_{50} = 1.7 μM and 1.3 μM, respectively), and these were comparable to the positive control 5-fluorouracil (IC_{50} = 1.8 μM).

Among the four salicylic acid series, SAR studies demonstrated that almost all the compounds belonging to the 5-iodo salicylic acid series showed the best activity both in the antiproliferative activities against Hep-G2 cell line and for EGFR inhibition. The results indicated that the iodine atom substituent at the 5-position could significantly increase the activity. Accordingly, compounds **22** and **28**, which contained an iodinated substituent at the 5-position, showed the best activity.

In every salicylic acid series, for instance a) salicylic acid series and c) 5-iodo salicylic acid series, substituents at the 2'-position could significantly increase the activity compared with substituents at the 4'-position [Table 1].

Furthermore, among these compounds where substituents took place at the 4'-position, electron-donating groups such as Me and *i*Pr groups, showed better activity than electron-withdrawing groups such as OMe, F, Cl and Br.

However, the SAR result summarised above was a brief overview of the whole 32 compounds synthesised, and for compound **28**, was a little different and seemed not to obey the SAR rule stated above. Docking simulations suggested that compound **28** had a good binding activity with EGFR kinase, and due to its chemical structure **28** was also a good EGFR inhibitor, and thus had good antiproliferative activity against *Hep-G2*.

Table 1. Physical Properties of salicylanilide derivatives **1**–**32**.

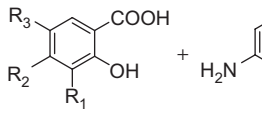

Compound	R_1	R_2	R_3	R_4	R_5	Formula	Mp °C	Yield, %
1	H	H	H	H	H	$C_{13}H_{11}NO_2$	127–129	74
2	H	H	H	F	H	$C_{13}H_{10}FNO_2$	120–122	78
3	H	H	H	Cl	H	$C_{13}H_{10}ClNO_2$	161–162	77
4	H	H	H	Br	H	$C_{13}H_{10}BrNO_2$	155–157	85
5	H	H	H	H	F	$C_{13}H_{10}FNO_2$	157–158	79
6	H	H	H	H	Cl	$C_{13}H_{10}ClNO_2$	157–159	83
7	H	H	H	H	Br	$C_{13}H_{10}BrNO_2$	159–161	71
8	H	H	H	F	F	$C_{13}H_9F_2NO_2$	183–185	75
9	H	H	H	Cl	Cl	$C_{13}H_9Cl_2NO_2$	191–193	70
10	H	H	H	H	CH_3	$C_{14}H_{13}NO_2$	145–147	81
11	H	H	H	H	OCH_3	$C_{14}H_{13}NO_3$	156–157	86
12	H	H	H	H	$CH(CH_3)_2$	$C_{16}H_{17}NO_2$	90–92	72
13	H	CH_3	H	H	H	$C_{14}H_{13}NO_2$	193–195	77
14	H	CH_3	H	Br	H	$C_{14}H_{12}BrNO_2$	165–167	83
15	H	CH_3	H	H	F	$C_{14}H_{12}FNO_2$	135–137	81
16	H	CH_3	H	H	Cl	$C_{14}H_{12}ClNO_2$	158–160	80
17	H	CH_3	H	F	F	$C_{14}H_{11}F_2NO_2$	196–198	71
18	H	CH_3	H	Cl	Cl	$C_{14}H_{11}Cl_2NO_2$	171–173	76
19	H	CH_3	H	H	CH_3	$C_{15}H_{15}NO_2$	154–156	73
20	H	CH_3	H	H	$CH(CH_3)_2$	$C_{17}H_{19}NO_2$	173–175	82
21	H	H	I	Cl	H	$C_{13}H_9ClINO_2$	194–195	85
22	H	H	I	Br	H	$C_{13}H_9BrINO_2$	181–182	70
23	H	H	I	H	F	$C_{13}H_9FINO_2$	230–232	81
24	H	H	I	H	Cl	$C_{13}H_9ClINO_2$	238–240	77
25	H	H	I	H	Br	$C_{13}H_9BrINO_2$	236–237	74
26	H	H	I	Cl	Cl	$C_{13}H_8Cl_2INO_2$	209–211	86
27	H	H	I	H	CH_3	$C_{14}H_{12}INO_2$	241–243	79
28	H	H	I	H	OCH_3	$C_{14}H_{12}INO_3$	232–234	75
29	Br	H	Br	H	F	$C_{13}H_8Br_2FNO_2$	204–205	85
30	Br	H	Br	H	Cl	$C_{13}H_8Br_2ClNO_2$	200–202	73
31	Br	H	Br	H	Br	$C_{13}H_8Br_3NO_2$	166–168	71
32	Br	H	Br	H	OCH_3	$C_{14}H_{11}Br_2NO_3$	153–155	82

Binding Mode of 22 and 28 into EGFR Kinase

To give an structural insight into the ligand/enzyme interactions, and to give an explanation and understanding of good activity observed, molecular docking of the most active compounds **22** and **28** into the ATP binding site of EGFR kinase, the binding model based on the EGFR complex structure (PDB code: 1M17, [10]) was performed using the automated docking tools AutoDock (version 4.0) [21–23]. The binding models of compounds **22** and **28** into EGFR were depicted in Figures 1 and 2.

Docking studies of both compounds **22** and **28** into the active site of EGFR provided well clustered solutions. In the binding model of compound **22** and EGFR, there was a hydrogen bond between the carbonyl oxygen of **22** and the N-H of the Lys828 side chain. Moreover, a cation-π interaction between the Lys828 side chain and the aniline ring (C1′, C2′, C3′, C4′, C5′, C6′ [Table 1]) of **22** was also observed. Cation-π interaction is a noncovalent molecular interaction between the face of an electron-rich π system (e.g. benzene, ethylene) with an adjacent cation. This unusual interaction is an example of noncovalent bonding between a monopole (cation) and a quadrupole (π system). Cation-π interaction energies are of the same order of magnitude as hydrogen bonds or salt bridges and play an important role in molecular recognition [24]. Cation-π interaction made the **22**/EGFR kinase complex more stable.

In the binding model of compound **28** and EGFR, there was also a cation-π interaction between the Lys828 side chain and the salicylic ring (C1, C2, C3, C4, C5 and C6 shown in Table 1) of **28**. Unexpectedly, there were two H-bonds observable for compound **28**: one between the N-H of **28** and the carboxylate of Gln767, and the other between the phenolic hydroxyl of **28** and the carboxylate of Gln767.

Table 2. Antiproliferative activity data and inhibition of EGFR kinase for the salicylanilide derivatives **1**–**32**.[a]

Compound	Antiproliferative effects against *Hep-G2* IC_{50} (μM)	EGFR inhibition IC_{50} (μM)
1	NA	>50
2	80 ± 28	24.83
3	52 ± 17	14.18
4	61 ± 10	21.92
5	246 ± 69	>50
6	137 ± 37	41.76
7	140 ± 38	>50
8	NA	>50
9	114 ± 28	45.29
10	84 ± 26	25.74
11	111 ± 21	39.98
12	82 ± 31	29.62
13	NA	>50
14	56 ± 13	22.19
15	110 ± 49	40.17
16	NA	>50
17	NA	>50
18	78 ± 17	31.09
19	104 ± 33	34.67
20	NA	>50
21	5.9 ± 1.3	4.37
22	1.7 ± 0.28	0.92
23	NA	>50
24	24 ± 3.5	13.04
25	24 ± 7.1	13.7
26	19 ± 2.5	9.66
27	5.1 ± 0.85	2.68
28	1.3 ± 0.2	0.63
29	154 ± 44	>50
30	22 ± 5.2	12.19
31	47 ± 16	28.53
32	37 ± 1	22.39
5-fluorouracil	1.8 ± 0.23	0.32

[a]NA, not active, the IC_{50} is greater than the maximal concentration tested (300 μM).

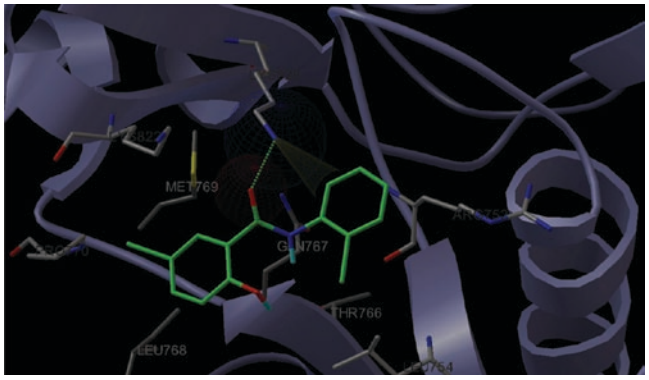

Figure 1. Binding mode of compound **22** with EGFR kinase. For clarity only the interacting residues were displayed. Ligand (green) and interacting key residues (white) were represented as stick models, while the proteins (white) were represented as ribbons. The H-bond was displayed as spherical surface, and the cation-π interaction was displayed as coniform surface.

In both cases, the binding was further stabilised by hydrophobic interactions between the phenyl group and a hydrophobic region, comprised of the side chains of Leu754, Thr766 and the Met769 side chains.

Conclusions

A series of salicylanilide derivatives were synthesised by reacting substituted salicylic acids and anilines then evaluated for antiproliferative activities against the human cancer cell line *Hep-G2*. Compounds **22** and **28** showed the most potent antiproliferative activities with IC_{50} values of 1.7 and 1.3 μM. The EGFR inhibitory ability of these synthesised salicylanilide derivatives were also evaluated using a solid-phase ELISA assay, which had almost the same trend as the antiproliferative activities assay. SAR results suggested that the substituents at the 5-position and 2'-position could increase the activity significantly. Docking simulations were performed to give the probable binding modes of compounds **22** and **28** into the ATP binding site of EGFR kinase. Compounds **22** and **28** both formed a cation-π interaction with Lys828 through their phenyl rings. However, compound **28** formed two H-bonds with Gln767 through its N-H and phenolic hydroxyl into the EGFR binding site, and compound **22** formed only one H-bond with Lys828 through its carbonyl oxygen. Still, both **22** and **28** could bind the EGFR kinase well. The result indicated that compounds **22** and **28**, in particular, had significant *Hep-G2* antiproliferative activities and EGFR inhibitory activity, and are promising potential agents for the treatment of liver cancer.

Experimental Section

Chemistry

All chemicals (reagent grade) used in the experiment were purchased from Aldrich (St. Louis, USA) and Sinopharm

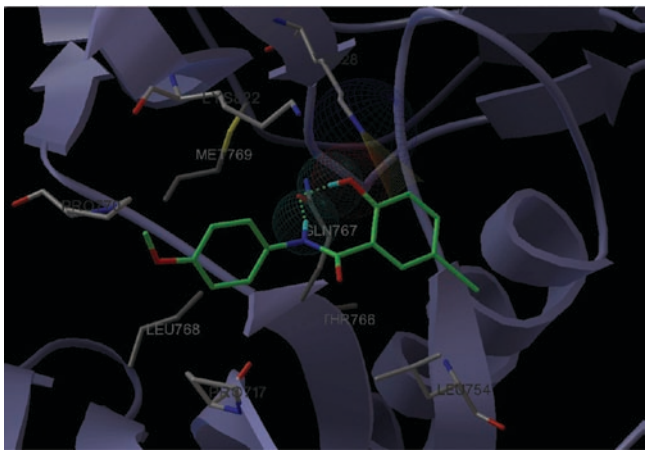

Figure 2. Binding mode of compound **28** with EGFR kinase. For clarity only the interacting residues were displayed. Ligand (green) and interacting key residues (white) were represented as stick models, while the proteins (white) were represented as ribbons. The H-bond was displayed as spherical surface, and the cation-π interaction was displayed as coniform surface.

Chemical Reagent (Shanghai, China). Melting points (uncorrected) were determined on a XT4 MP apparatus (Taike, Beijing). TLC was run on the silica gel coated aluminum sheets (silica gel 60 GF_{254},E. Merk, Darmstadt, Germany) and visualised in UV light (254 nm). EI spectra were obtained on a Waters GCT mass spectrometer (Illinois, USA), and ^{1}H NMR spectra were recorded on a Bruker DPX-300, AV-300 or AV-500 spectrometer (Rheinstetten, Germany) at 25 °C with TMS and solvent signals allotted as internal standards. Chemical shifts were reported in ppm (δ). Elemental analyses were performed on a CHN-O-Rapid instrument (Hanau, Germany) and were within ± 0.4 % of the theoretical values.

General method of synthesis 1–32

Equimolar quantities (1 mmol) of substituted salicylic acid and aniline were dissolved in CH_2Cl_2 (5 mL), and 1 mmol EDC (1-(3-Dimethylaminopropyl)-3-ethylcarbodiimide) were also added to the solution as catalyst. The solution was then stirred under refluxing for approximately 8 hours. The solvent was evaporated and the residue purified by column chromatography on silica gel, eluting with petroleum ether/EtOAc (3:1) to give a white, light yellow or brown solid of high purity with a good to high yield (70–86%).

2-Hydroxy-N-phenylbenzamide (1)

Light yellow powder, mp 127–129°C ^{1}H NMR (300 MHz, d_6-DMSO): 6.97 (t, J=8.3 Hz, 2H); 7.15 (t, J=7.5 Hz, 1H); 7.35–7.47 (m, 3H); 7.71 (d, J=7.7 Hz, 2H); 7.97 (dd, J_1=1.3 Hz, J_2=7.7 Hz, 1H); 10.37 (s, 1H); 11.79 (s, 1H). MS (ESI): 214.1 ($C_{13}H_{12}NO_2$, $[M+H]^+$). Anal. Calcd for $C_{13}H_{11}NO_2$: C, 73.23; H, 5.2; N, 6.57%; Found: C, 73.31; H, 5.17; N, 6.54%.

N-(2-fluorophenyl)-2-hydroxybenzamide (2)

White powder, mp 120–122°C ^{1}H NMR (300 MHz, d_6-DMSO): 7.03 (d, J=8.8 Hz, 2H); 7.16–7.36 (m, 3H); 7.43–7.48 (m, 1H); 8.03 (d, J=7.9 Hz, 1H); 8.18–8.24 (m, 1H); 10.69 (s, 1H); 11.91 (s, 1H). MS (ESI): 232.1 ($C_{13}H_{11}FNO_2$, $[M+H]^+$). Anal. Calcd for $C_{13}H_{10}FNO_2$: C, 67.53; H, 4.36; F, 8.22; N, 6.06%; Found: C, 67.42; H, 4.34; F, 8.26; N, 6.08%.

N-(2-chlorophenyl)-2-hydroxybenzamide (3)

White powder, mp 161–162°C ^{1}H NMR (500 MHz, d_6-DMSO): 7–7.05 (m, 2H); 7.17–7.2 (m, 1H); 7.37–7.41 (m, 1H); 7.44–7.48 (m, 1H); 7.56 (dd, J_1=1.5 Hz, J_2=8 Hz, 1H); 8.05 (dd, J_1=1.8 Hz, J_2=8 Hz, 1H); 8.39 (dd, J_1=1.5 Hz, J_2=8.2 Hz, 1H); 10.88 (s, 1H); 11.91 (s, 1H). MS (ESI): 248 ($C_{13}H_{11}ClNO_2$, $[M+H]^+$). Anal. Calcd for $C_{13}H_{10}ClNO_2$: C, 63.04; H, 4.07; Cl, 14.31; N, 5.66%; Found: C, 63.13; H, 4.02; Cl, 14.28; N, 5.69%.

N-(2-bromophenyl)-2-hydroxybenzamide (4)

White powder, mp 155–157°C ^{1}H NMR (500 MHz, d_6-DMSO): 6.99–7.05 (m, 2H); 7.11–7.14 (m, 1H); 7.41–7.48 (m, 2H); 7.71 (dd, J_1=1.6 Hz, J_2=8.3 Hz, 1H); 8.05 (dd, J_1=1.9 Hz, J_2=8 Hz, 1H); 8.3 (dd, J_1=1.6 Hz, J_2=8.3 Hz); 10.76 (s, 1H); 11.91 (s, 1H). MS (ESI): 293.9 ($C_{13}H_{11}BrNO_2$, $[M+H]^+$). Anal. Calcd for $C_{13}H_{10}BrNO_2$: C, 53.45; H, 3.45; Br, 27.35; N, 4.79%; Found: C, 53.52; H, 3.42; Br, 27.36; N, 4.75%.

N-(4-fluorophenyl)-2-hydroxybenzamide (5)

White powder, mp 157–158°C ^{1}H NMR (500 MHz, d_6-DMSO): 6.95–6.99 (m, 2H); 7.19–7.23 (m, 2H); 7.42–7.46 (m, 1H); 7.71–7.74 (m, 2H); 7.95 (dd, J_1=1.5 Hz, J_2=7.8 Hz, 1H); 10.39 (s, 1H); 11.75 (s, 1H). MS (ESI): 232.1 ($C_{13}H_{11}FNO_2$, $[M+H]^+$). Anal. Calcd for $C_{13}H_{10}FNO_2$: C, 67.53; H, 4.36; F, 8.22; N, 6.06%; Found: C, 67.61; H, 4.32; F, 8.24; N, 6.01%.

N-(4-chlorophenyl)-2-hydroxybenzamide (6)

Light yellow powder, mp 157–159°C ^{1}H NMR (300 MHz, d_6-DMSO): 6.99 (d, J=8.4 Hz, 2H); 7.43 (dd, J_1=1.8 Hz, J_2=7 Hz, 3H); 7.76 (dd, J_1=2 Hz, J_2=6.9 Hz, 2H); 7.93 (dd, J_1= 1.7 Hz, J_2=7.9 Hz, 1H); 10.44 (s, 1H); 11.63 (s, 1H). MS (ESI): 248.7 ($C_{13}H_{11}ClNO_2$, $[M+H]^+$). Anal. Calcd for $C_{13}H_{10}ClNO_2$: C, 63.04; H, 4.07; Cl, 14.31; N, 5.66%; Found: C, 62.98; H, 4.1; Cl, 14.29; N, 5.7%.

N-(4-bromophenyl)-2-hydroxybenzamide (7)

White powder, mp 159–161°C ^{1}H NMR (300 MHz, d_6-DMSO): 6.94–7 (m, 2H); 7.41–7.47 (m, 1H); 7.56 (d, J=8.8 Hz, 2H); 7.71 (d, J=8.8 Hz, 2H); 7.93 (d, J=7.9 Hz, 1H); 10.45 (s, 1H); 11.63 (s, 1H). MS (ESI): 293.1 ($C_{13}H_{11}BrNO_2$, $[M+H]^+$). Anal. Calcd for $C_{13}H_{10}BrNO_2$: C, 53.45; H, 3.45; Br, 27.35; N, 4.79%; Found: C, 53.5; H, 3.48; Br, 27.28; N, 4.77%.

N-(2,4-difluorophenyl)-2-hydroxybenzamide (8)

Brown powder, mp 183–185°C ^{1}H NMR (500 MHz, d_6-DMSO): 6.98–7.02 (m, 2H); 7.12–7.15 (m, 1H); 7.37–7.42 (m, 1H); 7.44–7.48 (m, 1H); 8.01 (dd, J_1=1.8 Hz, J_2=8.0 Hz, 1H); 8.09–8.13 (m, 1H); 10.58 (s, 1H); 11.89 (s, 1H). MS (ESI): 250.2 ($C_{13}H_{10}F_2NO_2$, $[M+H]^+$). Anal. Calcd for $C_{13}H_9F_2NO_2$: C, 62.65; H, 3.64; F, 15.25; N, 5.62%; Found: C, 62.58; H, 3.66; F, 15.19; N, 5.64%.

N-(2,4-dichlorophenyl)-2-hydroxybenzamide (9)

Light yellow powder, mp 191–193°C ^{1}H NMR (300 MHz, d_6-DMSO): 6.99–7.06 (m, 2H); 7.44–7.5 (m, 2H); 7.74 (d, J=2.4 Hz, 1H); 8.04 (d, J=7.9 Hz, 1H); 8.46 (d, J=8.8 Hz, 1H); 10.94 (s, 1H); 11.95 (s, 1H). MS (ESI): 283.1 ($C_{13}H_{10}Cl_2NO_2$, $[M+H]^+$). Anal. Calcd for $C_{13}H_9Cl_2NO_2$: C, 55.34; H, 3.22; Cl, 25.13; N, 4.96%; Found: C, 55.24; H, 3.23; Cl, 25.19; N, 4.99%.

2-Hydroxy-N-p-tolylbenzamide (10)

Light yellow powder, mp 145–147°C ^{1}H NMR (300 MHz, d_6-DMSO): 2.29 (s, 3H); 6.98 (d, J=7.7 Hz, 2H); 7.18 (d, J=8.2 Hz, 2H); 7.41-7.47 (m, 1H); 7.59 (d, J=8.4 Hz, 2H); 7.97 (d, J=8.2 Hz, 1H); 10.32 (s, 1H); 11.89 (s, 1H). MS (ESI): 228.3 ($C_{14}H_{14}NO_2$, $[M+H]^+$). Anal. Calcd for

$C_{14}H_{13}NO_2$: C, 73.99; H, 5.77; N, 6.16%; Found: C, 73.87; H, 5.79; N, 6.21%.

2-Hydroxy-N-(4-methoxyphenyl)benzamide (11)

White powder, mp 156–157°C ^{1}H NMR (500 MHz, d_6-DMSO): 3.76 (s, 3H); 6.94–6.97 (m, 4H); 7.42–7.45 (m, 1H); 7.6 (d, J = 9.2 Hz, 2H); 7.98 (d, J = 7.7 Hz, 1H); 10.27 (s, 1H); 11.99 (s, 1H). MS (ESI): 244.3 ($C_{14}H_{14}NO_3$, $[M+H]^+$). Anal. Calcd for $C_{14}H_{13}NO_3$: C, 69.12; H, 5.39; N, 5.76%; Found: C, 69.24; H, 5.34; N, 5.80%.

2-Hydroxy-N-(4-isopropylphenyl)benzamide (12)

White powder, mp 90–92°C ^{1}H NMR (300 MHz, d_6-DMSO): 1.21 (d, J = 7.0 Hz, 6H); 2.84–2.93 (m, 1H); 6.97 (d, J = 7.9Hz, 2H); 7.24 (d, J = 8.4 Hz, 2H); 7.41–7.46 (m, 1H); 7.61 (d, J = 8.4 Hz, 2H); 7.98 (d, J = 8.2 Hz, 1H); 10.31 (s, 1H); 11.89 (s, 1H). MS (ESI): 256.3 ($C_{16}H_{18}NO_2$, $[M+H]^+$). Anal. Calcd for $C_{16}H_{17}NO_2$: C, 75.27; H, 6.71; N, 5.49%; Found: C, 75.35; H, 6.68; N, 5.46%.

2-Hydroxy-4-methyl-N-phenylbenzamide (13)

White powder, mp 193–195°C ^{1}H NMR (300 MHz, d_6-DMSO): 2.31 (s, 3H); 6.79 (d, J = 4.9 Hz, 2H); 7.14 (t, J = 7.5 Hz, 1H); 7.37 (t, J = 8 Hz, 2H); 7.69 (d, J = 7.5 Hz, 2H); 7.91 (d, J = 8.4 Hz, 1H); 10.31 (s, 1H); 11.93 (s, 1H). MS (ESI): 228.3 ($C_{14}H_{14}NO_2$, $[M+H]^+$). Anal. Calcd for $C_{14}H_{13}NO_2$: C, 73.99; H, 5.77; N, 6.16%; Found: C, 73.87; H, 5.81; N, 6.19%.

N-(2-bromophenyl)-2-hydroxy-4-methylbenzamide (14)

White powder, mp 165–167°C ^{1}H NMR (500 MHz, d_6-DMSO): 2.31 (s, 3H); 6.81–6.84 (m, 2H); 7.1–7.13 (m, 1H); 7.4–7.43 (m, 1H); 7.70 (dd, J_1 = 1.5 Hz, J_2 = 8.3 Hz, 1H); 7.93 (dd, J_1 = 1.5 Hz, J_2 = 8 Hz, 1H); 8.29 (dd, J_1 = 1.5 Hz, J_2 = 8.3 Hz, 1H); 10.68 (s, 1H); 11.83 (s, 1H). MS (ESI): 307.2 ($C_{14}H_{13}BrNO_2$, $[M+H]^+$). Anal. Calcd for $C_{14}H_{12}BrNO_2$: C, 54.92; H, 3.95; Br, 26.1; N, 4.58%; Found: C, 55.01; H, 3.94; Br, 26.07; N, 4.59%.

N-(4-fluorophenyl)-2-hydroxy-4-methylbenzamide (15)

White powder, mp 135–137°C ^{1}H NMR (300 MHz, d_6-DMSO): 2.30 (s, 3H); 6.79 (d, J = 4.4 Hz, 2H); 7.21 (t, J = 9 Hz, 2H); 7.69–7.73 (m, 2H); 7.89 (d, J = 8.2 Hz, 1H); 10.34 (s, 1H); 11.9 (s, 1H). MS (ESI): 246.3 ($C_{14}H_{13}FNO_2$, $[M+H]^+$). Anal. Calcd for $C_{14}H_{12}FNO_2$: C, 68.56; H, 4.93; F, 7.75; N, 5.71%; Found: C, 68.69; H, 4.89; F, 7.72; N, 5.69%.

N-(4-chlorophenyl)-2-hydroxy-4-methylbenzamide (16)

White powder, mp 158–160°C ^{1}H NMR (300 MHz, d_6-DMSO): 2.3 (s, 3H); 6.79 (d, J = 6.4 Hz, 2H); 7.43 (dd, J_1 = 2 Hz, J_2 = 6.8 Hz, 2H); 7.75 (dd, J_1 = 2 Hz, J_2 = 6.8 Hz, 2H); 7.87 (d, J = 8.4 Hz); 10.4 (s, 1H); 11.79 (s, 1H). MS (ESI): 262.7 ($C_{14}H_{13}ClNO_2$, $[M+H]^+$). Anal. Calcd for $C_{14}H_{12}ClNO_2$: C, 64.25; H, 4.62; Cl, 13.55; N, 5.35%; Found: C, 64.31; H, 4.64; Cl, 13.49; N, 5.37%.

N-(2,4-difluorophenyl)-2-hydroxy-4-methylbenzamide (17)

Light yellow powder, mp 196–198°C ^{1}H NMR (300 MHz, d_6-DMSO): 2.3 (s, 3H); 6.81 (d, J = 5 Hz, 2H); 7.13 (t, J = 8.6 Hz, 1H); 7.35-7.43 (m, 1H); 7.91 (d, J = 8.4 Hz, 1H); 8.05-8.13 (m, 1H); 10.52 (s, 1H); 11.87 (s, 1H). MS (ESI): 264.2 ($C_{14}H_{12}F_2NO_2$, $[M+H]^+$). Anal. Calcd for $C_{14}H_{11}F_2NO_2$: C, 63.88; H, 4.21; F, 14.43; N, 5.32%; Found: C, 63.97; H, 4.18; F, 14.38; N, 5.29%.

N-(2,4-dichlorophenyl)-2-hydroxy-4-methylbenzamide (18)

White powder, mp 171–173°C ^{1}H NMR (500 MHz, d_6-DMSO): 2.31 (s, 3H); 6.85–6.87 (m, 2H); 7.2 (s, 1H); 7.26 (d, J = 8.0 Hz, 1H); 7.88–7.90 (m, 2H); 10.1 (s, 1H); 12.88 (br s, 1H). MS (ESI): 297.2 ($C_{14}H_{12}Cl_2NO_2$, $[M+H]^+$). Anal. Calcd for $C_{14}H_{11}Cl_2NO_2$: C, 56.78; H, 3.74; Cl, 23.94; N, 4.73%; Found: C, 56.7; H, 3.78; Cl, 23.99; N, 4.75%.

2-Hydroxy-4-methyl-N-p-tolylbenzamide (19)

Light yellow powder, mp 154–156°C ^{1}H NMR (300 MHz, d_6-DMSO): 2.29 (s, 3H); 2.3 (s, 3H); 6.78 (d, J = 4.8 Hz, 2H); 7.18 (d, J = 8.3 Hz, 2H); 7.57 (d, J = 8.4 Hz, 2H); 7.91 (d, J = 8.4 Hz, 1H); 10.24 (s, 1H); 12.02 (s, 1H). MS (ESI): 242.3 ($C_{15}H_{16}NO_2$, $[M+H]^+$). Anal. Calcd for $C_{15}H_{15}NO_2$: C, 74.67; H, 6.27; N, 5.81%; Found: C, 74.8 H, 6.22; N, 5.78%.

2-Hydroxy-N-(4-isopropylphenyl)-4-methylbenzamide (20)

White powder, mp 173–175°C ^{1}H NMR (300 MHz, d_6-DMSO): 1.21 (d, J = 7 Hz, 6H); 2.3 (s, 3H); 2.86–2.9 (m, 1H); 6.77–6.79 (m, 2H); 7.24 (d, J = 8.4 Hz, 2H); 7.6 (d, J = 8.6 Hz, 2H); 7.91 (d, J = 8.4 Hz, 1H); 10.28 (s, 1H); 12.04 (s, 1H). MS (ESI): 270.3 ($C_{17}H_{20}NO_2$, $[M+H]^+$). Anal. Calcd for $C_{17}H_{19}NO_2$: C, 75.81; H, 7.11; N, 5.20%; Found: C, 75.7; H, 7.16; N, 5.23%.

N-(2-chlorophenyl)-2-hydroxy-5-iodobenzamide (21)

Brown powder, mp 194–195°C ^{1}H NMR (500 MHz, d_6-DMSO): 7.02 (d, J = 8.5 Hz, 1H); 7.2 (t, J = 7.7 Hz, 1H); 7.4 (t, J = 7.7 Hz, 1H); 7.57 (d, J = 8 Hz, 1H); 7.62 (dd, J_1 = 2.5 Hz, J_2 = 8.5 Hz, 1H); 8.13 (d, J = 2.5 Hz, 1H); 8.38 (d, J = 8.2 Hz, 1H); 10.85 (s, 1H); 12.25 (s, 1H). MS (ESI): 374.6 ($C_{13}H_{10}ClINO_2$, $[M+H]^+$). Anal. Calcd for $C_{13}H_9ClINO_2$: C, 41.8; H, 2.43; Cl, 9.49; I, 33.97; N, 3.75%; Found: C, 41.72; H, 2.45; Cl, 9.53; I, 33.92; N, 3.77%.

N-(2-bromophenyl)-2-hydroxy-5-iodobenzamide (22)

Brown powder, mp 181–182°C ^{1}H NMR (500 MHz, d_6-DMSO): 7.02 (d, J = 8.8 Hz, 1H); 7.15 (t, J = 7.7 Hz, 1H); 7.44 (t, J = 7.7 Hz, 1H); 7.62 (dd, J_1 = 2.5 Hz, J_2 = 8.8 Hz, 1H); 7.72 (d, J = 8 Hz, 1H); 8.13 (d, J = 2.7 Hz, 1H); 8.29 (d, J = 8.2 Hz, 1H); 10.74 (s, 1H); 12.24 (s, 1H). MS (ESI): 419 ($C_{13}H_{10}BrINO_2$, $[M+H]^+$). Anal. Calcd for $C_{13}H_9BrINO_2$: C, 37.35; H, 2.17; Br, 19.11; I, 30.36; N, 3.35%; Found: C, 37.44; H, 2.16; Br, 19.08; I, 30.31; N, 3.37%.

N-(4-fluorophenyl)-2-hydroxy-5-iodobenzamide (23)

White powder, mp 230–232°C ^{1}H NMR (500 MHz, d_6-DMSO): 6.96 (d, J = 8.8 Hz, 1H); 7.22 (t, J = 8.8 Hz, 2H); 7.58 (dd, J_1 = 2.5 Hz, J_2 = 8.8 Hz, 1H); 7.7–7.73 (m, 2H); 8.07 (d, J = 2.5 Hz, 1H); 10.42 (s, 1H); 11.81 (s, 1H). MS (ESI): 358.1

($C_{13}H_{10}FINO_2$, $[M+H]^+$). Anal. Calcd for $C_{13}H_9FINO_2$: C, 43.72; H, 2.54; F, 5.32; I, 35.54; N, 3.92%; Found: C, 43.83; H, 2.52; F, 5.31; I, 35.59; N, 3.9%.

N-(4-chlorophenyl)-2-hydroxy-5-iodobenzamide (24)

White powder, mp 238–240°C ^{1}H NMR (500 MHz, d_6-DMSO): 6.96 (d, J=8.8 Hz, 1H); 7.43 (d, J=8.8 Hz, 2H); 7.58 (dd, J_1=2.5 Hz, J_2=8.8 Hz, 1H); 7.74 (d, J=8.8 Hz, 2H); 8.03 (d, J=2.5 Hz, 1H); 10.46 (s, 1H); 11.7 (s, 1H). MS (ESI): 374.6 ($C_{13}H_{10}ClINO_2$, $[M+H]^+$). Anal. Calcd for $C_{13}H_9ClINO_2$: C, 41.8; H, 2.43; Cl, 9.49; I, 33.97; N, 3.75%; Found: C, 41.72; H, 2.43; Cl, 9.52; I, 34.03; N, 3.78%.

N-(4-bromophenyl)-2-hydroxy-5-iodobenzamide (25)

White powder, mp 236–237°C ^{1}H NMR (500 MHz, d_6-DMSO): 6.97 (d, J=8.5 Hz, 1H); 7.55–7.59 (m, 3H); 7.69 (d, J=8.8 Hz, 2H); 8.03 (d, J=2.5 Hz, 1H); 10.45 (s, 1H); 11.7 (s, 1H). MS (ESI): 419 ($C_{13}H_{10}BrINO_2$, $[M+H]^+$). Anal. Calcd for $C_{13}H_9BrINO_2$: C, 37.35; H, 2.17; Br, 19.11; I, 30.36; N, 3.35%; Found: C, 37.49; H, 2.16; Br, 19.07; I, 30.4; N, 3.32%.

N-(2,4-dichlorophenyl)-2-hydroxy-5-iodobenzamide (26)

Brown powder, mp 209–211°C ^{1}H NMR (300 MHz, d_6-DMSO): 7.3 (d, J=8.8 Hz, 1H); 7.49 (dd, J_1=2.4 Hz, J_2=8.8 Hz, 1H); 7.63 (dd, J_1=2.7 Hz, J_2=8.6 Hz, 1H); 7.75 (d, J=2.4 Hz, 1H); 8.11 (d, J=2.6 Hz, 1H); 8.43 (d, J=8.8 Hz, 1H); 10.91 (s, 1H); 12.3 (s, 1H). MS (ESI): 409 ($C_{13}H_9Cl_2INO_2$, $[M+H]^+$). Anal. Calcd for $C_{13}H_8Cl_2INO_2$: C, 38.27; H, 1.98; Cl, 17.38; I, 31.1; N, 3.43%; Found: C, 38.41; H, 1.96; Cl, 17.35; I, 31.07; N, 3.44%.

2-Hydroxy-5-iodo-N-p-tolylbenzamide (27)

Light yellow powder, mp 241–243°C ^{1}H NMR (300 MHz, d_6-DMSO): 2.29 (s, 3H); 6.96 (d, J=8.8 Hz, 1H); 7.18 (d, J=8.2 Hz, 2H); 7.58 (dd, J_1=2.2 Hz, J_2=8.8 Hz, 3H); 8.1 (d, J=2.4 Hz, 1H); 10.34 (s, 1H); 11.95 (s, 1H). MS (ESI): 354.2 ($C_{14}H_{13}INO_2$, $[M+H]^+$). Anal. Calcd for $C_{14}H_{12}INO_2$: C, 47.61; H, 3.42; I, 35.93; N, 3.97%; Found: C, 47.72; H, 3.41; I, 35.87; N, 3.95%.

2-Hydroxy-5-iodo-N-(4-methoxyphenyl)benzamide (28)

White powder, mp 232–234°C ^{1}H NMR (300 MHz, d_6-DMSO): 3.76 (s, 3H); 6.95 (d, J=9 Hz, 3H); 7.56–7.61 (m, 3H); 8.12 (d, J=2.6 Hz, 1H); 10.31 (s, 1H); 12.04 (s, 1H). MS (ESI): 370.2 ($C_{14}H_{13}INO_3$, $[M+H]^+$). Anal. Calcd for $C_{14}H_{12}INO_3$: C, 45.55; H, 3.28; I, 34.38; N, 3.79%; Found: C, 45.43; H, 3.3; I, 34.45; N, 3.82%.

3,5-Dibromo-N-(4-fluorophenyl)-2-hydroxybenzamide (29)

Brown powder, mp 204–205°C ^{1}H NMR (500 MHz, d_6-DMSO): 7.25 (t, J=7.9 Hz, 2H); 7.68 (dd, J_1=5.2 Hz, J_2=7.9 Hz, 2H); 8.23 (s, 1H); 8.39 (s, 1H); 10.66 (s, 1H); 13.16 (br s, 1H). MS (ESI): 390 ($C_{13}H_9Br_2FNO_2$, $[M+H]^+$). Anal. Calcd for $C_{13}H_8Br_2FNO_2$: C, 40.14; H, 2.07; Br, 41.08; F, 4.88; N, 3.6%; Found: C, 40.22; H, 2.06; Br, 41.01; F, 4.86; N, 3.59%.

3,5-Dibromo-N-(4-chlorophenyl)-2-hydroxybenzamide (30)

Brown powder, mp 200–202°C ^{1}H NMR (500 MHz, d_6-DMSO): 7.47 (dd, J_1=2.1 Hz, J_2=6.8 Hz, 2H); 7.72 (dd, J_1=2.2 Hz, J_2=6.7 Hz, 2H); 8.02 (d, J=2.4 Hz, 1H); 8.26 (d, J=2.1 Hz, 1H); 10.72 (s, 1H); 12.72 (br s, 1H). MS (ESI): 406.5 ($C_{13}H_9Br_2ClNO_2$, $[M+H]^+$). Anal. Calcd for $C_{13}H_8Br_2ClNO_2$: C, 38.51; H, 1.99; Br, 39.41; Cl, 8.74; N, 3.45%; Found: C, 38.6; H, 1.99; Br, 39.37; Cl, 8.72; N, 3.44%.

3,5-Dibromo-N-(4-bromophenyl)-2-hydroxybenzamide (31)

Brown powder, mp 166–168°C ^{1}H NMR (500 MHz, d_6-DMSO): 7.46 (d, J=8.9 Hz, 2H); 7.71 (d, J=8.6 Hz, 2H); 8.24 (d, J=1.8 Hz, 1H); 8.37 (d, J=1.8 Hz, 1H); 10.71 (s, 1H); 13 (br s, 1H). MS (ESI): 450.9 ($C_{13}H_9Br_3NO_2$, $[M+H]^+$). Anal. Calcd for $C_{13}H_8Br_3NO_2$: C, 34.7; H, 1.79; Br, 53.28; N, 3.11%; Found: C, 34.81; H, 1.78; Br, 53.24; N, 3.09%.

3,5-Dibromo-2-hydroxy-N-(4-methoxyphenyl)benzamide (32)

Brown powder, mp 153–155°C ^{1}H NMR (500 MHz, d_6-DMSO): 3.77 (s, 3H); 6.98 (dd, J_1=2.2 Hz, J_2=6.8 Hz, 2H); 7.57 (dd, J_1=2.2 Hz, J_2=6.8 Hz, 2H); 8.01 (d, J=2.5 Hz, 1H); 8.31 (d, J=2.5 Hz, 1H); 10.56 (s, 1H); 13.25 (br s, 1H). MS (ESI): 402.1 ($C_{14}H_{12}Br_2NO_3$, $[M+H]^+$). Anal. Calcd for $C_{14}H_{11}Br_2NO_3$: C, 41.93; H, 2.76; Br, 39.85; N, 3.49%; Found: C, 42.01; H, 2.75; Br, 39.81; N, 3.47%.

Antiproliferative activities assay

The antiproliferative activities of the salicylanilide derivatives **1**–**32** were determined using a standard 3-(4,5-dimethylthylthiazol-2-yl)-2,5-diphenyltetrazolium bromide (MTT) colorimetric assay (Sigma, St. Louis, USA). Briefly, cell lines were seeded at a density of 7×10^3 cells/well in 96-well microtiter plates (Costar, Bethesda, USA). After 24 h, exponentially growing cells were exposed to the indicated compounds at final concentrations ranging from 0.5 to 300 μM, 5-fluorouracil was used as a positive control [25]. After 48 h, cell survival was determined by the addition of an MTT solution (10 μL of 5 mg/mL MTT in PBS). After 4 h, 100 μL of 10% SDS in 0.01 N HCl was added, and the plates were incubated at 37°C for a further 18 h; optical absorbance was measured at 570 nm on an LX300 Epson Diagnostic microplate reader (Offenburg, Germany). Survival ratios were expressed as a percentage with respect to untreated cells. IC_{50} values were determined from replicates of six wells from at least two independent experiments.

EGFR Inhibitory Assay

A 1.6 kb cDNA encoded for the EGFR cytoplasmic domain (EGFR-CD, amino acids 645–1186) were cloned into the baculoviral expression vector pFASTBacHTc. A sequence that encodes $(His)_6$ was located at the 5′ upstream to the EGFR sequence and Sf-9 cells were infected for three days for protein expression. The Sf-9 cell pellets were solubilised at 0°C in a buffer at pH 7.4 containing 50 mM HEPES,

10 mM NaCl, 1% Triton, 10 μM ammonium molybdate, 100 μM sodium vanadate, 10 μg/mL aprotinin, 10 μg/mL leupeptin, 10 μg/mL pepstatin, and 16 μg/mL benzamidine HCl for 20 min followed by 20 min centrifugation. The crude extract supernatant was passed through an equilibrated Ni-NTA superflow packed column (Qiagen, Hilden, Germany) and washed with 10 mM and then 100 mM imidazole to remove any nonspecifically bound material. The histidine tagged proteins were eluted with 250 and 500 mM imidazole and dialysed against 50 mM NaCl, 20 mM HEPES, 10% glycerol, and 1 μg/mL each of aprotinin, leupeptin, and pepstatin for 2 h. The entire purification procedure was performed at 4°C or on ice [26].

The EGFR kinase assay was set up to assess the level of autophosphorylation based on DELFIA/Time-Resolved Fluorometry. Compounds **1**–**32** were dissolved in 100% DMSO and diluted to the appropriate concentrations with 25 mM HEPES at pH 7.4. In each well, 10 μL of compound was incubated with 10 μL (12.5 ng for HER-2 or 5 ng for EGFR) of recombinant enzyme (1:80 dilution in 100 mM HEPES) for 10 min at room temperature. Then, 10 μL of 5 mM buffer (containing 20 mM HEPES, 2 mM $MnCl_2$, 100 μM Na_3VO_4, and 1 mM DTT) and 20 μL of 0.1 mM ATP-50 mM $MgCl_2$ was added for 1 h. Positive and negative controls were included in each plate by incubation of enzyme with or without ATP-$MgCl_2$. At the end of the incubation period, the liquid was aspirated, and plates were washed three times with wash buffer. A 75 μL (400 ng) sample of europium labeled anti-phosphotyrosine antibody was added to each well for a further 1 h of incubation. After washing, enhancement solution was added and the signal was detected by Victor (Wallac, Massachusetts, USA) with excitation at 340 nm and emission at 615 nm. The percentage of autophosphorylation inhibition by the compounds was calculated using the following equation: 100% - [(negative control)/(positive control- negative control)]. The IC_{50} was obtained from the percentage inhibition curves with eight concentrations of the compound. As the contaminants in the enzyme preparation are fairly low, the majority of the signal detected by the anti-phosphotyrosine antibody was from EGFR.

Docking Simulations

Molecular docking of compounds **22** and **28** into the three-dimensional EGFR complex structure (download from the Protein data Bank (PDB) PDB code: 1M17) was carried out using the AutoDock software package (version 4.0) as implemented through the graphical user interface AutoDockTools (ADT 1.4.6).Declaration of Interest

This work was supported by the Jiangsu National Science Foundation (No. BK2009239) and Anhui National Science Foundation (No. 070416274X).

References

1. Burkhart DJ, Barthel BL, Post GC, Kalet BT, Nafie JW, Shoemaker RK, Koch TH. Design, synthesis, and preliminary evaluation of doxazolidine carbamates as prodrugs activated by carboxylesterases. J Med Chem 2006;49:7002–7012.
2. Ksander GM, de Jesus R, Yuan A, Fink C, Moskal M, Carlson E, Kukkola P, Bilci N, Wallace E, Neubert A, Feldman D, Mogelesky T, Poirier K, Jeune M, Steele R, Wasvery J, Stephan Z, Cahill E, Webb R, Navarrete A, Lee W, Gibson J, Alexander N, Sharif H, Hospattankar A. Diaminoindanes as microsomal triglyceride transfer protein inhibitors. J Med Chem 2001;44:4677–4687.
3. Ou TM, Lu YJ, Zhang C, Huang ZS, Wang XD, Tan JH, Chen Y, Ma DL, Wong KY, Tang JCO, Chan ASC, Gu LQ. Stabilization of G-quadruplex DNA and down-regulation of oncogene *c-myc* by quindoline derivatives. J Med Chem 2007;50:1465–1474.
4. Hsieh PW, Chang FR, Wu CC, Wu KY, Li CM, Chen SL, Wu YC. New cytotoxic cyclic peptides and dianthramide from *Dianthus superbus.* J Nat Prod 2004;67:1522–1527.
5. Fry DW, Kraker AJ, McMichael A, Ambroso LA, Nelson JM, Leopold WR, Connors RW, Bridges AJ. A specific inhibitor of the epidermal growth factor receptor tyrosine kinase. Science 1994;265:1093–1995.
6. Ward WHJ, Cook PN, Slater AM, Davies DH, Holdgate GA, Green LR. Epidermal growth factor receptor tyrosine kinase. Investigation of catalytic mechanism, structure based searching and discovery of a potent inhibitor. Biochem Pharmacol 1994;48:659–666.
7. Tsou HR, Mamuya N, Johnson BD, Reich MF, Gruber BC, Ye F, Nilakantan R, Shen R, Discafani C, DeBlanc R, Davis R, Koehn FE, Greenberger LM, Wang YF, Wissner A. 6-Substituted-4-(3-bromophenylamino) quinazolines as putative irreversible inhibitors of the epidermal growth factor receptor (EGFR) and human epidermal growth factor receptor (HER-2) tyrosine kinases with enhanced antitumor activity. J Med Chem 2001;44:2719–2734.
8. Bridges AJ, Zhou H, Cody DR, Rewcastle GW, McMichael A, Showalter HDH, Fry DW, Kraker AJ, Denny W. Tyrosine kinase inhibitors 8. An unusually steep structure-activity relationship for analogues of 4-(3-bromoanilino)-6,7-dimethoxyquinazoline (PD 153035), a potent inhibitor of the epidermal growth receptor. J Med Chem 1996;39:267–276.
9. Domarkas J, Dudouit F, Williams C, Qiyu Q, Banerjee R, Brahimi F, Jean-Claude BJ. The combi-targeting concept: synthesis of stable nitrosoureas designed to inhibit the epidermal growth factor rceptor (EGFR). J Med Chem 2006;49:3544–3552.
10. Kamath S, Buolamwini JK. Receptor-guided alignment-based comparative 3D-QSAR studies of benzylidene malonitrile tyrphostins as EGFR and HER-2 kinase inhibitors. J Med Chem 2003;46:4657–4668.
11. Brahimi F, Matheson SL, Dudouit F, McNamee JP, Tari AM, Jean-Claude BJ. Inhibition of epidermal growth factor receptor.mediated signaling by "combi-triazene" BJ2000, a new probe for combi-targeting postulates. J Pharmacol Exp Ther 2002;303:238–246.
12. Matheson SL, McNamee J, Jean-Claude BJ. Design of a chimeric 3-methyl-1,2,3-triazene with mixed receptor tyrosine kinase and DNA damaging properties: a novel tumor targeting strategy. J Pharmacol Exp Ther 2001;296:832–840.
13. Hickey K, Grehan D, Reid IM, O'Briain S, Walsh TN, Hennessy TPJ. Expression of epidermal growth-factor receptor and proliferating cell nuclear antigen predicts response of neophageal squamous-cell carcinoma to chemoradiotherapy. Cancer 1994;74:1693–1698.
14. Yarden Y, Sliwkowski MX. Untangling the ErbB signalling network. Mol Cell Biol 2001;2:127–137.
15. Hynes NE, Stern DF. The biology of ErbB-2 neu her-2 and its role in cancer. Biochim Biophys Acta 1994;1198:165–184.
16. Gullick WJ. Prevalence of aberrant expression of the epidermal growth-factor receptor in human cancers. Br Med Bull 1991;47:87–98.
17. Moscatello DK, Holgado-Mudruga M, Godwin AK, Ramirez G, Gunn G, Zoltick PW, Biegel JA, Hayes RL, Wong AJ. Frequent expression of a mutant epidermal growth-factor receptor in multiple human tumors. Cancer Res 1995;55:5536–5539.
18. Wikstrand CJ, McLendon RE, Friedman A, Bigner DD. Cell surface localization and density of the tumor-associated variant of the epidermal growth factor receptor, EGFRvIII. Cancer Res 1997;57:4130–4140.

19. Bridges AJ. The rationale and strategy used to develop a series of highly potent, irreversible, inhibitors of the epidermal growth factor receptor family of tyrosine kinases. Curr Med Chem 1999;6:825–843.
20. Boschelli DH. Small molecule inhibitors of receptor tyrosine kinases. Drugs Future 1999;24:515–537.
21. Morris GM, Goodsell DS, Halliday RS, Huey R, Hart WE, Belew RK, Olson AJ. Automated docking using a Lamarckian genetic algorithm and an empirical binding free energy function. J Comput Chem 1998;19:1639–1662.
22. Goodsell DS, Morris GM, Olson AJ, Automated docking of flexible ligands: applications of AutoDock. J. Mol. Recognit. 1996;9,1–5.
23. Huey R, Morris GM, Olson AJ, Goodsell DS. A semiempirical free energy force field with charge-based desolvation. J Comput Chem 2007;28:1145–1152.
24. Pless SA, Millen KS, Hanek AP, Lynch JW, Lester HA, Lummis SCR, Dougherty DA. A cation-pi interaction in the binding site of the glycine receptor is mediated by a phenylalanine residue. J Neurosci 2008;28:10937–10942.
25. Xiao ZP, Li HQ, Shi L, Lv PC, Song ZC, Zhua HL. Synthesis, antiproliferative activity, and structure-activity relationships of 3-aryl-1H-quinolin-4-ones. Chem Med Chem 2008;3:1077–1082.
26. Tsou HR, Mamuya N, Johnson BD, Reich MF, Gruber BC, Ye F, Nilakantan R, Shen R, Discafani C, DeBlanc R, Davis R, Koehn FE, Greenberger LM, Wang YF, Wissner A. 6-Substituted-4-(3-bromophenylamino)quinazolines as putative irreversible inhibitors of the epidermal growth factor receptor (EGFR) and human epidermal growth factor receptor (HER-2) tyrosine kinases with enhanced antitumor activity. J Med Chem 2001;44:2719–2734.